COMBINED TORSIONAL AND ELECTROMECHANICAL ANALYSIS OF AN LNG COMPRESSION TRAIN WITH VARIABLE SPEED DRIVE SYSTEM

by

Paola Rotondo
Senior Electrical Engineer
GE Oil & Gas
Florence, Italy

Davide Andreo
R&D Engineer
ABB Medium Voltage Drives
Turgi, Switzerland

Stefano Falomi
Ph.D. Student
University of Florence, Italy

Pieder Jörg
Vice President Drives Projects
ABB Medium Voltage Drives
Turgi, Switzerland

Andrea Lenzi
Senior Engineer
GE Oil & Gas
Florence, Italy

Tim Hattenbach
Senior Principal Mechanical Engineer and Compressor Team Leader
Bechtel Corporation
Houston, Texas

Duccio Fioravanti
Design Engineer
and
Sergio De Franciscis
Lead Electrical Engineer
GE Oil & Gas
Florence, Italy

Paola Rotondo is currently a Senior Electrical Engineer and Variable Speed Drives Systems Team Leader in the Electrical Department of GE Oil & Gas, in Florence, Italy. She joined GE in 2005 and is involved in requisition activities, string test support, and system simulations for several projects. Before joining GE, she was a researcher at Centro Laser, Valenzano, Italy, where she worked on the development of numerical and experimental medical and industrial models by using rapid prototyping techniques.

Dr. Rotondo received M.Sc. and Ph.D. degrees (Electrical Engineering) from Politecnico di Bari, Bari, Italy, in 2003 and 2007, respectively.

Davide Andreo is an R&D Engineer at ABB Medium Voltage Drives, in Turgi, Switzerland. His main activities focus on electrical drive simulation and motor control software.

Mr. Andreo received his M.Sc. degree (Mechatronics Engineering, 2008) from the Politecnico di Torino, Italy.

Stefano Falomi is currently a Ph.D. Student at Florence University, sponsored by GE Oil & Gas. His activities focus on torsional vibrations of turbomachines and torsional interactions between compressor trains and electrical power systems.

Mr. Falomi received his M.Sc. degree (Mechanical Engineering, 2007) from the University of Florence.

Pieder Jörg is Vice President Drives Projects, for ABB Medium Voltage Drives, in Turgi, Switzerland. He is responsible for the drive systems business. He joined ABB in 1995, starting at Corporate Research in the area of power electronics. In 2002 he joined the Medium Voltage Drives business unit as Head of Product Development. Since 2008 he has been responsible for the Drive Systems business and its products within Medium Voltage Drives.

Mr. Jörg received his M.Sc. degree (Electrical Engineering) from the Swiss Federal Institute of Technology.

Andrea Lenzi is a Senior Engineer in the Electrical Design Department at GE Oil & Gas, in Florence, Italy. He supports the electrical design department in risk review of critical jobs, system integration, reliability review, and supplier technical quality coordination. He covered the position of Project Engineer for North Sea projects from 2002 to 2006 and coordinated the development of a very large VSDS compressor application for the Ormen Lange project. He is also involved in implementation of Lessons Learned in GE Oil & Gas Electrical Drives Design.

Mr. Lenzi received his M.Sc. degree (Chemical Engineering, 1997) from Pisa University.

Timothy J. (Tim) Hattenbach is Senior Principal Mechanical Engineer and Compressor Team Leader with Bechtel Corporation in their Houston, Texas office. He has worked for Bechtel for 31 years and has 35 years of experience in the oil and gas industry. He has been the responsible engineer for full load string tests from 10 MW to 85 MW.

Mr. Hattenbach has B.S. and M.S. degrees (Mechanical Engineering, 1972, 1974) from the University of Houston. He is a contributor to the Bechtel LNG Product Development Center and staff consultant on machinery issues. Mr. Hattenbach is the Taskforce Chairman for API Standards 670 (Machinery Protection Systems) and 616 (Gas Turbines), and is a member of the API 692 Taskforce for Compressor Gas Seals. Mr. Hattenbach is a registered Professional Engineer in the State of Texas.

Duccio Fioravanti is a Design Engineer in the Mechanical Auxiliary Systems GEAR team for GE Oil & Gas, in Florence, Italy. He joined them in 2007, and his work mainly concerns gearboxes and coupling selections for different oil and gas applications. He has been a reviewer for international journals and conferences on robotic topics.

Dr. Fioravanti received his M.Sc. degree (Mechanical Engineering, 2004) from the University of Florence and his Ph.D. degree (Applied Mechanics, 2008) from the University of Bologna. His research activities mainly concerned visual serving, robot control, and multibody dynamics in railway systems.

Sergio De Franciscis is a Lead Electrical Engineer in the Electrical Department of GE Oil & Gas in Florence, Italy. He joined GE in 2007, working on several projects using variable speed electrical drives. Before joining GE, he worked for five years in the design of control systems and electronic hardware for power electrical conversion.

Mr. De Franciscis received his M.Sc. degree (Electronics) from the Politecnico di Torino, Italy.

ABSTRACT

Nowadays variable speed drive systems (VSDS) are preferred to constant speed drives in the oil and gas industry because they can improve the efficiency of the process while avoiding the use of complex mechanical mechanisms (e.g., guide vanes) or plant recycling and throttling. However, the reputation of VSDS has not always been favorable since they can be a cause of torsional vibration problems. This is mainly due to the intrinsic nature of switching-based electrical systems to produce pulsating torque ripple on the shaft. In addition, closed-loop electromechanical interactions could lead to system instability. The aim of this paper is to introduce a new combined approach to deal with torsional phenomena, especially in high shaft-power applications such as liquefied natural gas (LNG) trains. Besides the conventional shaft-line modal analysis, a precise understanding of the electromechanical interactions is achieved through combined simulations between the shaft-line designer (compressor manufacturer) and the VSDS supplier together with a full-load-full-speed (FLFS) train string test. Simulations and string test results confirmed satisfactory torsional behavior and electromechanical stability of the overall system.

INTRODUCTION

One of the major improvements in the efficiency of plant operations in the oil and gas industry has been the use of variable speed drive systems (VSDS) where the Electric Motor speed can be adjusted to maximize the efficiency of the overall system, avoiding the use of complex mechanical mechanisms (e.g., guide vanes) or plant recycling and throttling (Baccani, 2007; Miranda and Brick, 2004).

VSDS are employed mainly in the following oil and gas industry applications: LNG trains, pipelines, reinjection, storage recompression, subsea, and process gas compression. However, the use of VSDS is not free of concerns, in particular for high shaft-power applications. Disregarding specific issues typical of certain VSDS technologies (operability range, speed/torque control philosophy, etc.), two main critical aspects must be carefully considered: shaft torsional behavior and electromechanical interactions between the VSDS and the shaft-line. Typical problems of uncontrolled torsional vibrations are coupling failures, broken shafts, worn gears, fractured gear teeth, all of which result in undesired plant shutdowns (Kocur and Corcoran, 2008; Shimakawa and Kojo, 2007).

The key to avoiding these consequences is designing the entire shaft-line employing a precise understanding of the forcing torsional phenomena, including the selection of couplings, gearboxes, and rotors from a torsional standpoint. Excitation of torsional natural frequencies may come from many sources that may or may not be a function of running speed (e.g., aerodynamic excitations, misalignment effects, etc.) (API 684, 2005). Moreover, systems including a VSDS, unlike those using conventional constant speed electrical equipment, show a pulsating torque ripple on the shaft-line that is created by the switching nature of the VSDS itself.

This paper presents an overview of a new combined approach applied to an LNG application that includes a VSDS and is aimed at preventing torsional issues. Torsional phenomena are taken into account in the design phase of the shaft-line and the possible sources of torsional vibrations are simulated to assess the reliability of the design.

The structure of this paper follows the main steps of this approach. The train configuration described in the SYSTEM DESCRIPTION section, is composed of a gas turbine, three centrifugal compressors (multistage, horizontally split type) and an induction motor fed by a converter. Shaft-line modal analysis, including evaluation of possible excitations within the operating range, is performed in the MECHANICAL MODEL DESCRIPTION section. The VSDS working principles and related phenomena are considered in the ELECTRICAL SYSTEM DESCRIPTION AND MODELING section. Open loop and closed loop electromechanical simulations are reported in the SYSTEM SIMULATIONS part. Finally, in the EXPERIMENTAL RESULTS AND DISCUSSION section, the torsional behavior of the compressor train is validated with string test experimental results. Some final remarks and future opportunities are discussed in the CONCLUSIONS.

SYSTEM DESCRIPTION

The LNG train considered in this investigation consists of a 56,000 hp (42 MW) gas turbine, three centrifugal compressors, and a 9000 hp (6.6 MW) electric motor fed by a 9 MVA converter (rated torque ~ 10,000 lbf-ft (13,000 Nm), rated speed ~ 5000 rpm).

For this specific application, the electric motor is needed as additional source of starting torque due to the high absorbed torque by the train during startup which is due to the considerable shaft-line length typical of a single shaft mechanical drive gas turbine. An overview of the train is shown in Figure 1. The specific components of the train identified in Figure 1 are defined in Table 1.

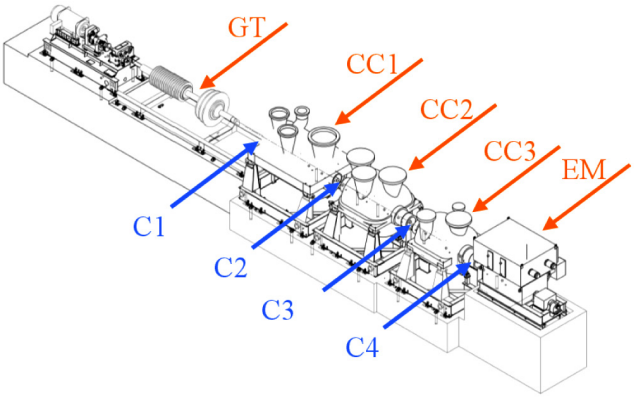

Figure 1. LNG Train Overview.

Table 1. Shaft-Line Abbreviations Used in this Paper.

Item	Meaning
GT	Gas turbine
CC1	Low pressure centrifugal compressor
CC2	Intermediate pressure centrifugal compressor
CC3	High pressure centrifugal compressor
EM	Electric motor
C1	Gas turbine drive end side coupling
C2	Coupling between low and intermediate pressure compressors
C3	Coupling between intermediate and high pressure compressors
C4	Electric motor drive end side coupling

To better validate the closed loop behavior of the entire electromechanical system during the string test phase, both mechanical and electrical measurements were performed. A dedicated data acquisition system (DAS) was set up to acquire, record, and monitor in real time both electrical and mechanical parameters including the mechanical torque (average and ripple) acting on the train shafts. These data were used for post processing analysis and comparison with simulation results. Particular attention was focused on:

- Electric motor currents and voltages that were acquired by means of external probes and were used to calculate the motor air-gap torque (AGT).
- Mechanical torque on coupling C4 (measured with a strain gauge [Norton, 1982]) and on coupling C2 (measured using a phase shift method [Gindy]).

The torque on coupling C4 was monitored since it is the torque transferred by the electric machine (EM) to the shaft-line. The torque on coupling C2 was monitored as well because it is where the first mode shape (which is usually the most problematic in electromechanical interactions [Lambrecht and Kulig, 1982]) has a nodal point (Figure 2). On the nodal point of each mode shape there is the highest pulsating torque response at the related torsional natural frequencies (TNF).

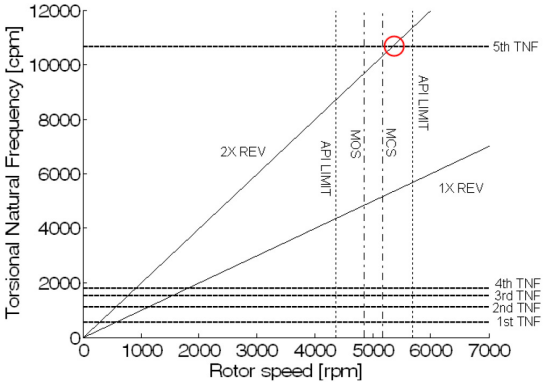

Figure 2. Mode Shapes Related to the First Four TNFs: Normalized Amplitude Versus Train Section.

MECHANICAL MODEL DESCRIPTION

In order to describe the torsional behavior of the system, a lumped elements model was developed following the recommendations of API 684 (2008) and API 617 (2002). The train was divided into 60 rigid inertias connected by massless torsional springs. This allows a proper description of the stiffness of each shaft section, including coupling connections and shrink fits.

Modal Analysis

Torsional natural frequencies of the system were calculated, performing an eigenanalysis on the equations of motion (modal analysis). In the modal analysis, damping is not considered since the low structural damping does not significantly affect the value of resonant frequencies and mode shapes (Walker, 2003). The equations, in matrix form, are the following:

$$[J]\ddot{\underline{\theta}} + [K]\underline{\theta} = \underline{0} \tag{1}$$

where $[J]$ is the diagonal inertia matrix and $[K]$ is the tridiagonal stiffness matrix. The vector $\underline{\theta}$ contains the degrees of freedom of the system, which are the rotations of each section about the shaft axis. The system is underconstrained, so there exists a zero solution, which is related to the rigid body motion of rotation. The nonzero solutions are the TNFs. The modal shapes related to the first four TNFs are plotted in Figure 3.

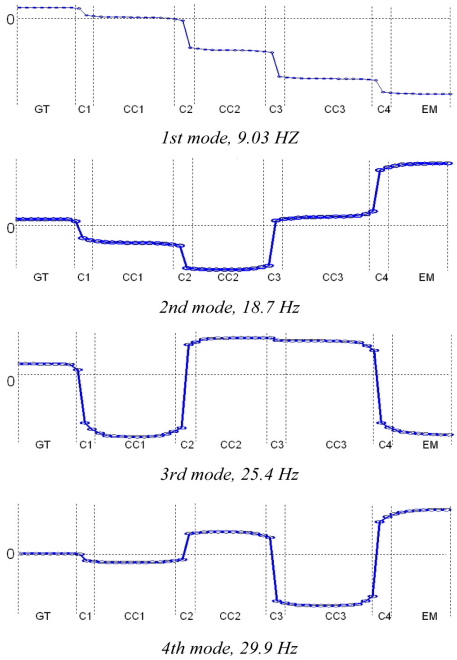

Figure 3. Campbell Diagram.

The interaction in the operating range between TNFs and possible torsional mechanical excitation are represented in the Campbell diagram (Walker, 2003) of Figure 2. Torsional excitations included in this diagram are those at 1× rev (synchronous excitations due to centrifugal compressors) and 2× rev (related to misalignments of couplings). API Standards (API 684, 2005) require that TNFs of the full train are at least 10 percent above or 10 percent below any possible excitation frequency within the specified operating speed range (minimum operating speed [MOS], maximum continuous speed [MCS]). These limits are defined in Figure 2 by two dashed vertical lines labeled API LIMITS.

The 2× rev crosses a TNF in this range (red circle in Figure 2). Fatigue verifications show that torsional stresses due to this excitation are considerably lower than the endurance limits of shafts and couplings. Couplings are selected to be the least stiff shaft-line components. As a consequence, the first four mode shape deformations are concentrated in the couplings, while the machines' shafts are not significantly deformed. Therefore the first four TNFs are mainly a function of coupling stiffness and machine inertia (API 684, 2005).

Forced Response

In order to perform a forced analysis, a mechanical damping term is included by means of the damping matrix [*C*]. Vector $\underline{T}$ contains external torques applied on the shafts.

$$[J]\underline{\ddot{\theta}} + [C]\underline{\dot{\theta}} + [K]\underline{\theta} = \underline{T} \tag{2}$$

Approximations of the Model

The resulting model does not take into account damping nonlinearities, e.g., effects such as elastic saturation and torsio-flexural interactions. None of the secondary excitations described in API 684 (2005), e.g., aerodynamic forces and misalignments effects, are included, nor is the interaction with the train's speed regulator considered.

Reduced Model

A closed loop simulation of the electromechanical system would have a heavy computational burden if the entire lumped parameter model were to be included. A modal reduction model was created, replacing the physical state variables with the amplitude of vibration for each torsional mode. Using the mass normalized modal matrix (Gatti and Ferrari) and assuming that the damping matrix is a linear combination of the inertia and stiffness matrices, the equation of motion for the i^{th} torsional mode is expressed as:

$$\ddot{s}_i + {}_i\frac{\omega_i}{AF_i}\dot{s}_i + {\omega_i}^2 s_i = \underline{\varphi}_i \cdot \underline{T} \tag{3}$$

where s_i is the modal amplitude of vibration, ω_i and $\underline{\varphi}_i$ are the natural frequency and mode shape for the i^{th} vibration mode calculated from undamped analysis, and AF_i is the modal amplification factor that was assumed based on experience on similar applications.

The reduced model is limited to the first four flexible modes for the following primary reasons:

- The first four modes do not involve shaft deformations, so they are less damped than those at higher frequency (Walker, 2003).
- Only the modes below the maximum continuous speed were considered (Ooi, 1981).
- Only the TNFs below the bandwidth of the drive (~100 Hz) were considered.
- From the fifth to the eighth mode shapes, the amplitude of the deformed on the EM section is negligible, so they cannot be excited by electric motor torque components.

Based on these criteria, modes higher than the fourth TNF were disregarded in the dynamics of the coupled electromechanical system included in this paper.

ELECTRICAL SYSTEM DESCRIPTION AND MODELING

The electrical drive system used in this application is a medium voltage VSDS based on direct torque control (DTC) technology. A 36-pulse diode rectifier supplies three floating DC-links, which are combined via the insulated gate commutated thyristor (IGCT)-based inverter output bridge in series. This topology (Figure 4), combined with a particular switching concept, provides a nine-level line-to-line output waveform of 6.6 kV, which feeds a three-phase squirrel cage induction motor of 9000 hp (6.6 MW) nominal power and 5100 rpm rated speed.

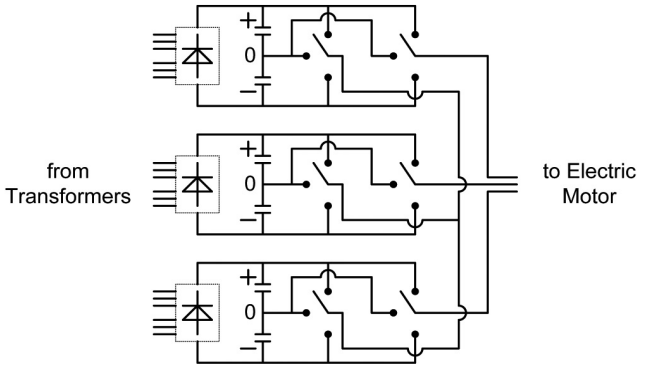

Figure 4. Functional Representation of the Electrical Topology of the Nine-Level Line-to-Line Output Inverter.

The frequency converter controls the operation of the motor by variation of frequency and voltage. In order to control speed and power, the frequency converter receives a torque set point from the train's speed regulator. The drive control platform employs DTC technology. This control scheme allows field orientation without feedback using advanced motor theory to calculate the motor torque directly; the controlling variables are motor magnetizing flux and motor torque (Tiitinen, et al., 1995). Based on the actual status of the torque and flux in the machine, the best suited voltage vector is selected. The frequency at which the power elements switch is therefore variable. The switching frequency value mainly influences the thermal losses in the power stages and the quality of the output waveform. Its value is controlled defining a tolerance band in which the torque and flux are acceptable through the so-called hysteresis controllers. Figure 5 shows the basic principle of a hysteresis based controller: *ht1* and *hf1* define, respectively, the bands in which the torque and the flux are considered to be acceptable.

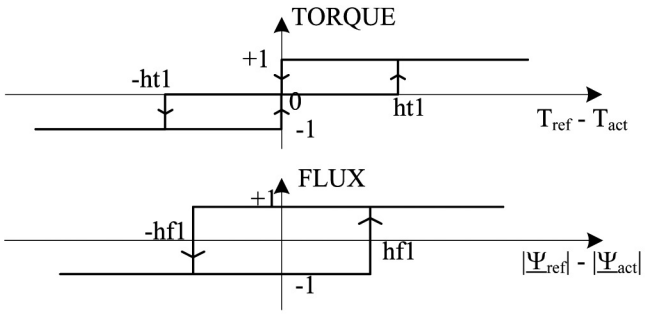

Figure 5. Representation of the Hysteresis Based Strategy of the DTC.

The main benefits of DTC technology are better torque response, torque control at low frequencies, and static and dynamic speed accuracy. Moreover, a fundamental feature in turbomachinery applications is that the produced air gap torque does not have any significant components in the low frequency range, thereby reducing the risk of exciting the torsional natural frequencies of the train.

The investigation related to this paper makes use of a detailed model of the electric drive including the supply of the converter, the power stages, the squirrel cage induction machine with flux saturation and skin effect model, the DTC control, and the measurement of control signals. The model is definitely nonlinear, taking into account switching elements, saturations, hysteresis bands, measurement resolution, discrete implementation of control algorithms, etc. The model of a one-mass mechanical system (the motor rotor) together with a load model is also a part of the simulator. The latter allows the selection of a square, linear, or constant speed torque curve. Figure 6 shows the simulator structure where $[v_a\ v_b\ v_c]$ are the three-phase voltages applied on the induction machine, $[V_{DC}\ i_a\ i_b\ i_c]$ are the measured values of the DC-link voltage together with inverter currents used by the control, $[g_u\ g_v\ g_w]$ are the applied switching commands, T_{airgap} is the air-gap torque produced by the induction machine, T_{load} is the load torque obtained by the load model, Ω_{motor} is the motor speed, and *Ref* is the external reference for the electric drive that could be either speed or torque. In the application considered in this paper, the external reference is a torque set point.

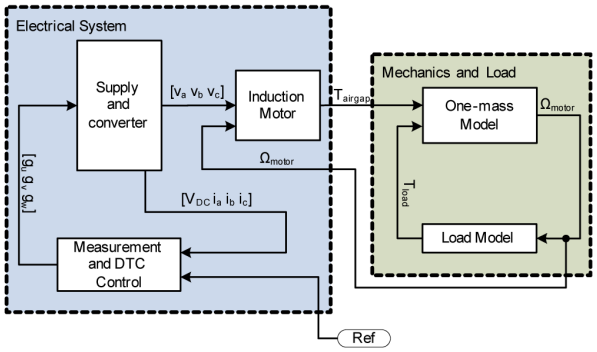

Figure 6. Block Structure of the Model of the Electric Drive and the Mechanical Load.

The simulations of the above described model use an integration algorithm based on a modified Rosenbrock formula of order two (Runge-Kutta 23), which is a one-step solver usually used for stiff problems (Shampine and Reichelt, 1997). The maximum allowed step size is set to 25μs, which is also the base for the simulation of the DTC control algorithm and the measurement and data acquisition system.

SYSTEM SIMULATIONS

Open Loop Analysis

In order to understand if any torque harmonic component of the VSDS drive could excite the mechanical system, an open loop simulation was carried out. The motor air-gap torque obtained from the VSDS simulator is the input of the modal model obtained in the MECHANICAL MODEL DESCRIPTION section. The air-gap torque was calculated with the electrical system driving only the motor (one-mass model of Figure 6) and for the following significant operating points (steady-state analysis):

- Rated torque, rated speed
- Rated torque, minimum operating speed (95 percent of rated)
- 50 percent of rated torque, rated Speed

The cyclic torques were calculated for the couplings and shaft sections, including stress concentration factors, and were compared to endurance fatigue limits for shafts (Walker, et al., 2003; Peterson), and to coupling supplier data.

Assessment of the fatigue life of the couplings requires the definition of the peak-to-peak amplitude of the load cycle. A conservative assumption is to define this amplitude as the difference between the maximum and minimum stresses obtained in simulation (Shigley), as showed in Figure 7. This amplitude is compared with the maximum allowable cyclic torque for infinite life operation (endurance limit) derived from the Goodman diagram (Shigley). The cyclic stresses in open loop simulations are well below the acceptable values for infinite life operation.

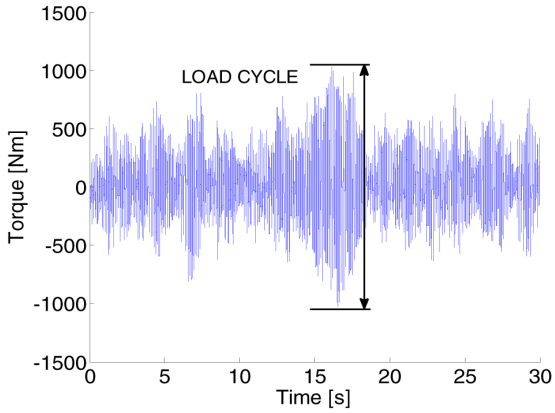

Figure.7. Oscillating Torque in C2 Coupling in Open Loop Simulation.

Closed Loop Simulations

In order to have higher confidence in the train's torsional performance and to investigate the electromechanical coupled behavior, a closed loop simulation was performed. A closed loop simulation takes into account the fact that the speed oscillations of the electric motor are seen by the electrical system as an oscillation of counter electromotive force. This leads to oscillating currents and so to oscillating torques, which are seen by the DTC as a disturbance in the inner torque control loop. In principle, any current or torque controller will react on this phenomenon. It must be ensured that the control is damping the oscillations and not exciting them, and this can be done only in a closed loop analysis.

In the combined model, the one-mass model sets the operating point while the alternating part is taken into account by the reduced modal model. The output of the modal model was therefore added to the output of the one-mass mechanical model (the motor rotor) and was included in the full drive model; a quadratic load model was selected, as usually done, on first approximation, for modeling compressor load characteristics. The output of the one-mass mechanical system is the continuous (steady-state) component of the motor speed, while the output of the modal model describes the components with alternating behavior. The motor speed is the input of the train speed regulator that produces a torque set point, i.e., the input of the drive model (Figure 7). The train speed regulator was modeled as a proportional-integral (PI) controller with a high time constant.

Figure 8 shows this configuration, where T_{airgap} is the air-gap torque, C_{motor} is the continuous component of the motor speed, Δ_{motor} is the oscillating part of the motor speed, Ω_{motor} is the motor speed (the sum of the previous two components), T_{load} is the load component from the load model, and T_{ref} is the torque set point for the electrical drive model.

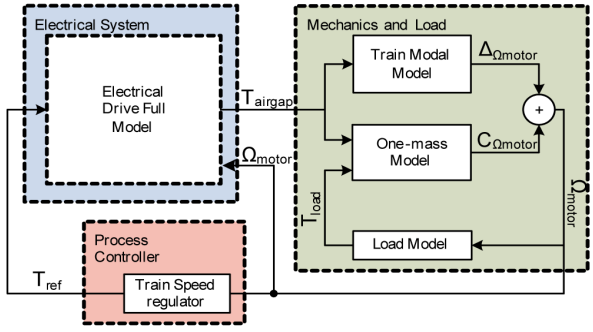

Figure 8. Electromechanical Model Simulator.

Using the above described model, a steady-state, full power condition was analyzed as was a transient condition where the load was raised in a single step from zero to 100 percent. A 25μs data sample time was chosen, corresponding to the maximum step size of the solver (more details on the solver used are provided in the ELECTRICAL SYSTEM DESCRIPTION AND MODELING section). Both the electrical and mechanical quantities were monitored. Particular attention was placed on the torque on coupling C2 (refer to the SYSTEM DESCRIPTION section for details). Figure 9 shows its trend, limited to the alternating part.

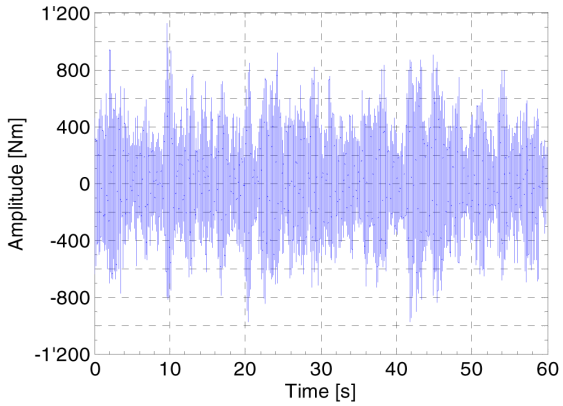

Figure 9. Simulation Results for the Alternating Torque on Coupling C2 Plotted Versus Time in a Steady-State Full Power Condition (1 Nm = 0.74 lbf-ft).

The frequency components of the signal were analyzed through a time waterfall plot of the spectra (Figure 10). A waterfall plot consists of a series of spectra calculated at consecutive times and is broadly used in the rotating machinery field since it shows how the amplitude of frequency components changes in time (Randall). The abscissa displays frequency, the ordinate axis shows the time, and the third axis is the amplitude. The spectra were calculated for a two second window, thus achieving a frequency resolution of:

$$f_{\min} = \frac{1}{T_{window}} = \frac{1}{2s} = 0.5Hz \tag{4}$$

which is the minimum frequency that could be detected. Moreover, an overlapping method was applied in order to maximize the use of the entire data set. Overlapping is a method that uses a percentage of the previous data block to calculate the spectra of the current data block (Randall). In this analysis, a $T_{window}/2$ overlap was used.

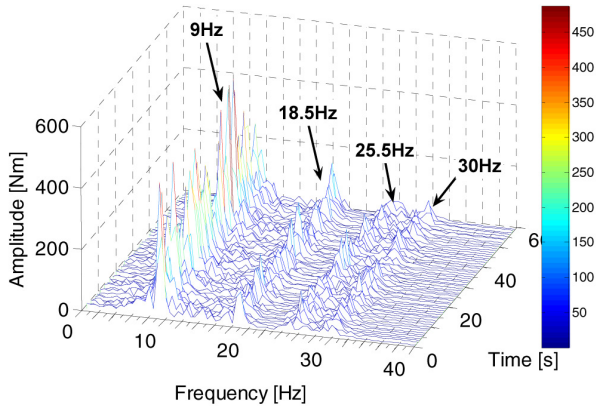

Figure 10. Time Waterfall Plot of the Spectra of the Simulated Alternating Torque on Coupling C2 in a Steady-State Full Power Condition (1 Nm = 0.74 lbf-ft).

As expected, the most notable components are those corresponding to the natural frequencies of the train. The air-gap torque components of the electric drive are amplified by the amplification factor of the mechanical train at those particular frequency values. Since a detailed model of the electrical system was used, certain frequency components could be observed around the TNFs; the order of magnitude of these components is, however, far from that of the TNFs.

Figure 11 shows a typical trend of the air-gap torque produced by the electric drive. Figure 12 shows that the spectrum is broadband, with low amplitude across the range that includes the first four TNFs; no characteristic frequencies can be detected.

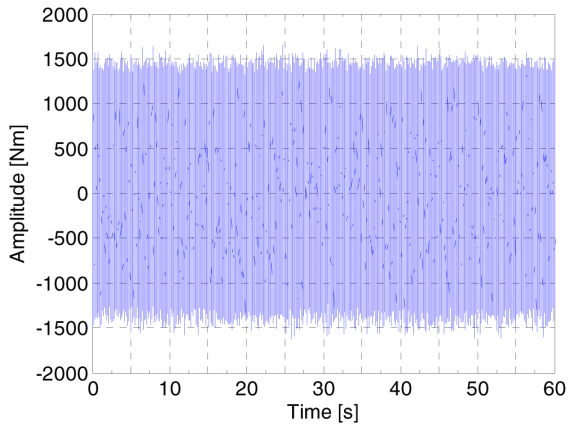

Figure 11. Simulated Air-Gap Alternating Torque Produced by the Electric Drive Plotted Versus Time in a Steady-State Full Power Condition (1 Nm = 0.74 lbf-ft).

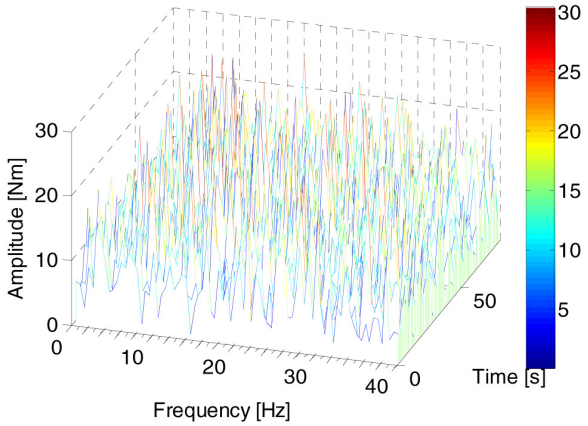

Figure 12. Time Waterfall Plot of the Spectra of the Simulated Air-Gap Torque in a Steady-State Full Power Condition (1 Nm = 0.74 lbf-ft).

To verify the closed loop behavior in terms of torsional stability, the step response of the system was simulated. This is recommended because the closed loop system torsional damping could differ from that of open loop. If the overall damping becomes negative, the system stability is no longer guaranteed. Since a typical scenario in a real application would be the discharging and charging of the compressors when the train is already rotating at full speed, a load step from rated value to zero and then back to rated value was simulated while the speed of the train was kept at the nominal value by the gas turbine.

Figure 13 shows the simulated results of torque on coupling C2 versus time during a load step toward zero (first transient) and a step toward the nominal value (second transient). The decay rate of torsional oscillation, directly related to the overall system damping factor, is mainly due to the assumed mechanical damping. The VSDS does not give a negative contribution to the closed loop stability.

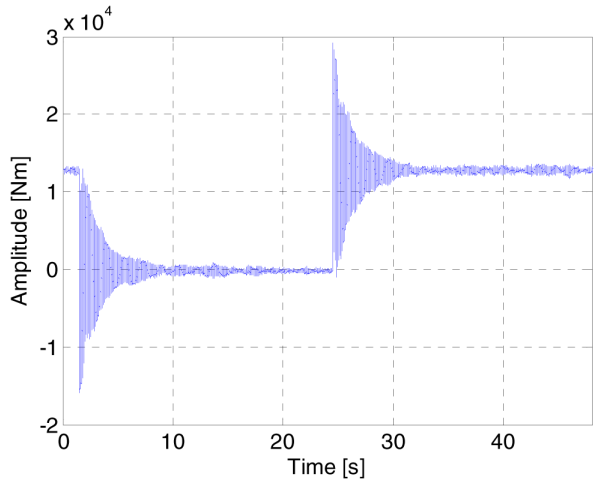

Figure 13. Simulated Torque on Coupling C2 Versus Time During a Load Step Toward Zero (First Transient) and a Step Toward the Nominal Value (Second Transient).

For both steady-state and step response conditions, the simulations show good behavior of the DTC regarding oscillating phenomena. The torque control loop of the electric drive is robust with respect to torsional oscillation disturbances of the train. The electrical system does not react to excite the oscillations, as may be seen by the time waterfall of the air-gap torque (Figure 12), which does not contain any significant harmonics at the natural frequencies of the mechanical train.

EXPERIMENTAL RESULTS AND DISCUSSION

This section reports a selection of experimental data collected during the string test of the electromechanical system. Particular attention was focused on three different conditions:

- VSDS off and gas turbine as the only source of power
- Electric drive and gas turbine both providing power
- Torque step request to the drive by the train speed regulator

Since in the simulator the power coming from the gas-turbine was not taken into account, the use of Nm instead of a normalized unit of measurement helps in making coherent comparisons. The test data sample frequency is 12,800 Hz and the signal processing methods used are the same as those employed in the SYSTEM SIMULATIONS section.

VSDS Off Operation

The condition of VSDS off was taken into account to quantify phenomena not directly related to the electric drive. Since in the combined model other sources of mechanical excitation are not included, the analysis of this operating condition is fundamental to making a coherent comparison between the simulation results and experimental data. Figure 14 shows the trend of the alternating part of the torque on the second coupling where the torque sensor was mounted. The spectra of this signal were analyzed using the time waterfall of Figure 15.

Steady-State Operation with VSDS at Full Load

This set of experimental data belongs to a condition of steady-state in which both the turbine and the drive are supplying power to the mechanical shaft. The main difference from the simulations performed in the SYSTEM SIMULATIONS section is that the electric drive is not the only source of torsional excitation; secondary mechanical causes, for example aerodynamic excitations, are also present. Figure 16 shows the trend of the alternating part of the torque on the C2 coupling, while Figure 17 presents its spectra.

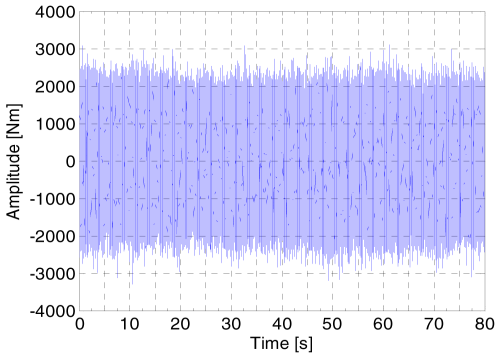

Figure 14. Measurement of the Alternating Torque on Coupling C2 Plotted Versus Time with the Electric Drive Applying No Torque (1 Nm = 0.74 lbf-ft).

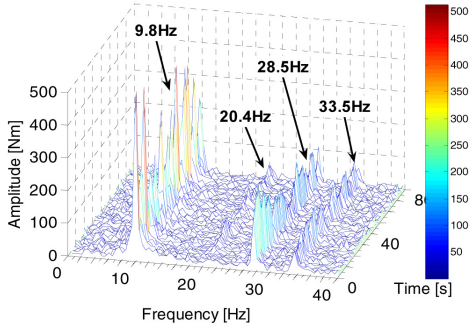

Figure 15. Time Waterfall Plot of the Spectra of the Measured Alternating Torque on Coupling C2 with the Electric Drive Applying No Torque (1 Nm = 0.74 lbf-ft).

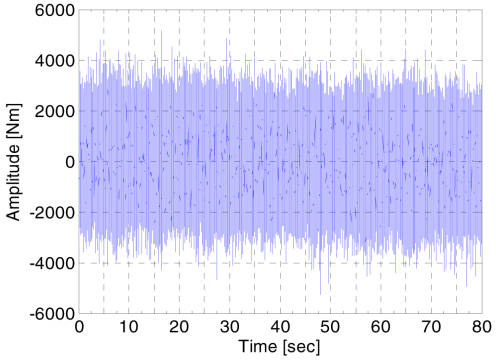

Figure 16. Measurement of the Alternating Torque on Coupling C2 Plotted Versus Time in a Steady-State Full Power Condition (1 Nm = 0.74 lbf-ft).

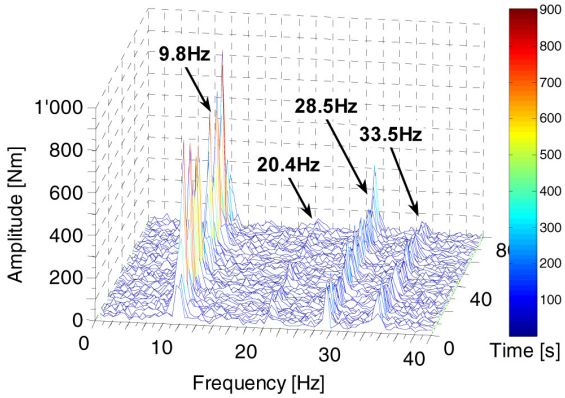

Figure 17. Time Waterfall Plot of the Spectra of the Measured Alternating Torque on Coupling C2 in a Steady-State Full Power Condition (1 Nm = 0.74 lbf-ft).

The air-gap torque was calculated from the measured motor phase currents and voltages. Figure 18 shows its trend in the time domain, while Figure 19 contains the time waterfall of its spectra. This result is comparable to that obtained through simulations (Figure 12) and confirms how the air-gap torque produced by the electrical system does not contain significant harmonics at the natural frequencies of the mechanical train.

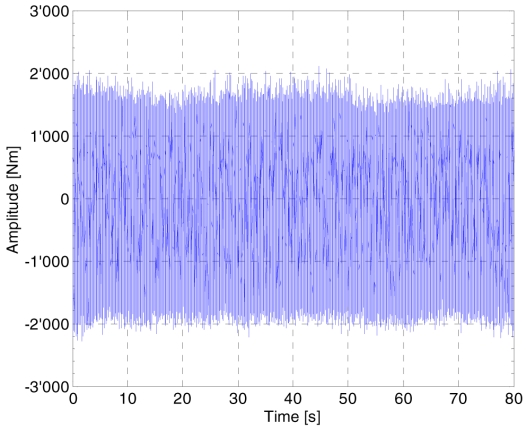

Figure 18. Calculated Air-Gap Alternating Torque Produced by the Electric Drive Plotted Versus Time in a Steady-State Full Power Condition (1 Nm = 0.74 lbf-ft).

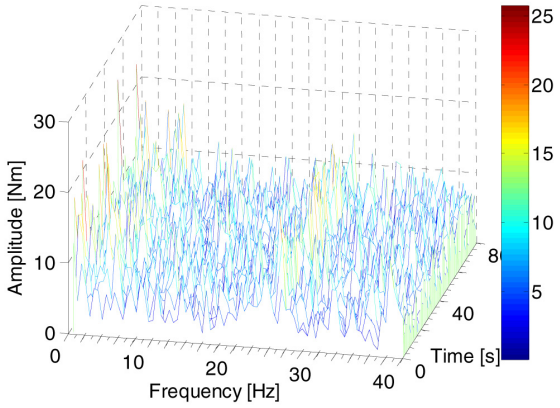

Figure 19. Time Waterfall Plot of the Spectra of the Calculated Air-Gap Alternating Torque Produced by the Electric Drive in a Steady-State Full Power Condition (1 Nm = 0.74 lbf-ft).

The analysis of steady-state experimental data (Figure 17) exhibits some differences from simulation results in terms of alternating torque response. In particular, referring to the amplitude of the simulated first natural frequency component (Figure 10), this higher value can be explained by the fact that other sources of excitation were not included in the model (e.g., aerodynamic effects in centrifugal machines). These excitation terms are not usually considered in the analysis since they have low magnitude components over a wide spectrum and they rarely create problems for fatigue life. Furthermore, a difference between experimental and simulation results can be noticed in the second torsional component amplitudes; this would need additional investigation.

Transient Analysis

The following experimental data refer to an electrical torque request from the train speed regulator following a steep ramp. While the train was rotating at full speed, the electric drive produced a torque from zero to the nominal value in approximately 5 seconds. As a result, coupling C2 is subjected to a torque as shown in Figure 20. This confirms the stability of the electromechanical system.

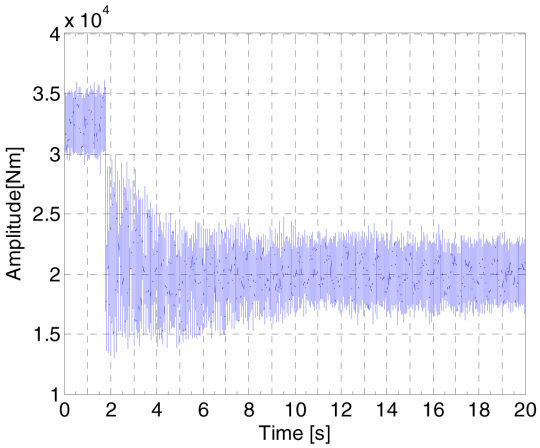

Figure 20. Measurement of the Torque on Coupling C2 Plotted Versus Time During a Steep Torque Ramp Request to the Electric Drive (1 Nm = 0.74 lbf-ft).

The counterintuitive reduction in the torque transmitted by the C2 coupling is due to the action of the train speed regulator. As the torque set point for the EM goes from zero to the rated torque, the gas turbine's output torque is reduced in order to keep the train speed constant. The differences in the average torques shown in Figure 13 are due to the absence of the train speed regulator in the closed loop models, or in other words, the turbine torque. Figure 20 shows that oscillations are damped, and the stability of the electromechanical system is confirmed.

CONCLUSIONS

In this work the authors have considered the torsional behavior related to electromechanical interactions in LNG applications. Standard torsional mechanical verifications and open loop simulations of the torsional stresses of the train are augmented with closed loop simulations including a detailed model of the electric drive that reproduces the main phenomena related to VSDS.

The results obtained during simulations were compared with results from an extensive FLFS string test campaign, which provided the opportunity to evaluate the approximation of the coupled model. In particular, it was verified that damping nonlinearities, secondary causes of train excitations, and interaction with the train's speed regulator do not have significant effects on the electromechanical system stability for this specific application. Moreover, it was noted that the impact of this particular VSDS topology and control on the train torsional behavior is of the same order of magnitude as that caused by train mechanical and secondary excitations (Wachel and Szenasi, 1993). The importance of the presented approach is proportional to the train power, operating speed, and mechanical complexity of the application.

The main contribution of this paper is to demonstrate that an understanding of electromechanical interactions is fundamental in the design phase of a compressor train and that it can only be achieved through a strong synergy between the manufacturers of the train components and the owners of the process and train. A further improvement of the methodology presented would be the inclusion of the primary nonlinearities in the simulation model, in particular for applications where their effect may not be negligible.

NOMENCLATURE

VSDS = Variable speed drive system
FLFS = Full load full speed string test
TNF = Torsional natural frequency
LNG = Liquefied natural gas
[J] = Inertia matrix
[K] = Stiffness matrix
[C] = Damping matrix

$\underline{\theta}$ = Rotation of shaft sections
$\underline{T}$ = Vector of external torques
s_i = Amplitude of torsional mode vibration
ω_i = Frequency of torsional mode
φ_i = Torsional mode shape
AF_i = Modal amplification factor, AF=1/(2ξ)
ξ = Modal damping (percent)
GT = Gas turbine
CC1 = Low pressure centrifugal compressor
CC2 = Intermediate pressure centrifugal
CC3 = High pressure centrifugal compressor
EM = Electrical motor
C1 = Gas turbine drive end side coupling
C2 = Coupling between low and intermediate pressure compressors
C3 = Coupling between intermediate and high pressure compressors
C4 = Electric motor drive end side coupling
DAS = Data acquisition system
AGT = Air gap torque
MOS = Minimum operating speed
MCS = Maximum continuous speed
DTC = Direct torque control
DC = Direct current
IGCT = Insulated gate commutated thyristor
$[v_a v_b v_c]$ = Three-phase voltages applied on the induction machine
$[V_{DC}]$ = DC-link voltage
$[i_a\ i_b\ i_c]$ = Inverter currents used by the DTC control
$[g_u g_v g_w]$ = Switching commands
T_{airgap} = Air-gap torque produced by the induction machine
T_{load} = Load torque obtained by the load model
Ω_{motor} = Electrical motor speed
Ref = External reference
C_{motor} = Continuous component of the electrical motor speed
Δ_{motor} = Oscillating part of the electrical motor speed

REFERENCES

API Standard 617, 2002, "Axial and Centrifugal Compressors and Expander-Compressors for Petroleum, Chemical and Gas Industry Services," Seventh Edition, American Petroleum Institute, Washington, D.C.

API Standard 684, 2005, "Tutorial on Rotordynamics: Lateral Critical, Unbalance Response, Stability, Train Torsional and Rotor Balancing," Second Edition, American Petroleum Institute, Washington, D.C.

Baccani, R., Zhang, R., Toma, T., Iuretig, A., and Perna, M., 2007, "Electric Systems for High Power Compressor Trains in Oil and Gas Applications—System Design, Validation Approach, and Performances," *Proceedings of the Thirty-Sixth Turbomachinery Symposium*, Turbomachinery Laboratory, Texas A&M University, College Station, Texas, pp. 61-68.

Gatti, P. L. and Ferrari, V., "Applied Structural and Mechanical Vibrations."

Genta, G., *Vibration of Structures and Machines—Practical Aspects*, Second Edition, Springer-Verlag.

Gindy, S. S., "Force and Torque Measurements, A Technology Overview Part Two—Torque," Wiley InterScience, *Experimental Techniques*, *9*, (7).

Kocur, J. Jr., and Corcoran, J. P., 2008, "VFD Induced Coupling Failure," Case Study Presented at the Thirty-Seventh Turbomachinery Symposium, Houston, Texas.

Lambrecht, D. and Kulig, T., 1982, "Torsional Performance of Turbine-Generator Shafts Especially under Resonant Excitation," IEEE Transactions on Power Apparatus and Systems, *PAS-101*, (10).

Miranda, M. A. and Brick, E. S., 2004, "Life Cycle Cost Assessment of Turbomachinery for Offshore Applications," *Proceedings of the Thirty-Third Turbomachinery Symposium*, Turbomachinery Laboratory, Texas A&M University, College Station, Texas, pp. 77-84.

Norton, H. N., 1982, *Sensor and Analyzer Handbook*, Prentice Hall.

Ooi, B. T., 1981, "Phase Modulation Theory of Electromechanical Damping in Synchronous Generator," IEEE Transactions on Power Apparatus and Systems, *PAS-100*, (5).

Peterson, R. E., *Stress Concentration Factors*, New York, New York: Wiley and Sons.

Randall, R. B., *Frequency Analysis*, Third Edition, Naerum, Denmark: Bruel & Kjaer.

Shampine, L. F. and Reichelt, M. W., 1997, "The MATLAB ODE Suite," SIAM Journal on Scientific Computing, *18*, pp. 1-22.

Shigley, J. E., "Mechanical Engineering Design," ASME Transactions, McGraw Hill Series in Mechanical Engineering.

Shimakawa, T. and Kojo, T., 2007, "The Torsional Torque Fluctuations of Compressor Train with Vector Control PWM Inverter," Case Study Presented at the Thirty-Sixth Turbomachinery Symposium, Houston, Texas.

Tiitinen, P., Pohjalainen, P., and Lalu, J., 1995, "Next Generation Motor Control Method: Direct Torque Control (DTC)," EPE Journal, *5*, (1), pp. 14-17.

Wachel, J. C. and Szenasi, F. R., 1993, "Analysis of Torsional Vibrations in Rotating Machinery," *Proceedings of the Twenty-Second Turbomachinery Symposium*, Turbomachinery Laboratory, Texas A&M University, College Station, Texas, pp. 127-152.

Walker, D., 2003, *Torsional Vibration of Turbo-Machinery*, McGraw-Hill.

Walker, D. N., Adams, S. L., and Placek, R. J., 1981, "Torsional Vibration and Fatigue of Turbine-Generator Shafts," IEEE Transactions on Power Apparatus and Systems, *PAS-100*, (11).

BIBLIOGRAPHY

ABB, "Drive ACS5000—Medium Voltage AC Drive for Control of Motors up to 6.9 kV," ABB technical documentation, 3BHT 490 501 R0001.

Hütten, V., Zurowski, R. M., and Hilscher, M., 2008, "Torsional Interharmonic Interaction Study of 75 MW Direct-Driven VSDS Motor Compressor Trains for LNG Duty," *Proceedings of the Thirty-Seventh Turbomachinery Symposium*, Turbomachinery Laboratory, Texas A&M University, College Station, Texas, pp. 57-66.

ACKNOWLEDGEMENT

The authors would like to thank the Advanced Technology/GE Oil & Gas Technology Laboratory, Test Data Analysis team, the GE Oil & Gas Eng Rotordynamics team, and the GE Oil & Gas ENG PA EDES for their support during the tests and during the data analysis.

The authors would also like to thank the GE Oil & Gas Auxiliary System Engineering GEAR team for the support provided in modeling the mechanical part of the system and in verifications of coupling fatigue. In addition the authors would like to thank the System Simulations group of ABB Medium Voltage Drives for their support in the simulations of the VSDS.